A closed-loop type algorithm for determination of variable blank holder force trajectory and its application to square cup deep drawing

著者	Kitayama Satoshi, Hamano Satoshi, Yamazaki Koetsu, Kubo Tatsuo, Nishikawa Hikaru, Kinoshita Hiroshi
journal or publication title	International Journal of Advanced Manufacturing Technology
volume	51
number	5-8
page range	507-517
year	2010-01-01
URL	http://hdl.handle.net/2297/26232

doi: 10.1007/s00170-010-2656-9

A Closed-loop Type Algorithm for Determination of Variable Blank Holder Force Trajectory and its Application to Square Cup Deep Drawing

Satoshi Kitayama[1], Satoshi Hamano[2], Koetsu Yamazaki[3], Tatsuo Kubo[4], Hikaru Nishikawa[5], Hiroshi Kinoshita[5]

[1] *Kanazawa University, Kakuma-machi, Kanazawa, 920-1192, Japan*

+81-76-234-4758

kitagon@t.kanazawa-u.ac.jp (Corresponding Author)

[2] *Graduate School of Natural Science & Technology, Kanazawa University, Kakuma-machi, Kanazawa, 920-1192, Japan*

[3] *Kanazawa University, Kakuma-machi, Kanazawa, 920-1192, Japan*

[4] *Komatsu Ltd., 5 Yookaichimatchijigata, Komatsu, 923-8666, Japan*

[5] *Komatsu Industries Corp., 5 Yookaichimatchijigata, Komatsu, 923-8666, Japan*

Abstract

In deep drawing, a low blank holder force (BHF) can cause wrinkling, while a high BHF can lead to tearing. Thus, it is important to determine the appropriate BHF to be utilized in the forming process. In this study, a variable blank holder force (VBHF) approach to deep drawing is employed, and a simple closed-loop type algorithm is developed to obtain the VBHF trajectory. The proposed algorithm is divided into two phases. The objective of the first phase is to check wrinkling and tearing. In this phase, a low BHF, which is the causes of wrinkling, is used as the initial BHF; it is then increased to prevent wrinkling. The algorithm is terminated when tearing occurs. In a numerical simulation, the distance between the die and the blank holder is used to measure wrinkling. On the other hand, the thickness of the blank is used to determine the tearing. Next, in the second phase, the deviations in thickness are examined. Wrinkles are also checked in the second phase. By iterating the above two phases, the VBHF trajectory can be obtained. One of the advantages of the VBHF is that it reduces the forming energy. The validity of the proposed algorithm is examined through both a numerical simulation and experiment.

Keywords: Variable Blank Holder Force, Deep Drawing, Numerical Simulation, Closed-loop Type Algorithm

Abbreviations

BHF: Blank holder force.

VBHF: Variable blank holder force.

FLD: Forming limit diagram.

RSM: Response surface methodology.

PI: Proportional plus integral.

PID: Proportional-integral-derivative.

ARSM: Adaptive response surface methodology.

ARMA: Auto-regressive moving-average.

FEA: Finite element analysis.

SPFC: Steel plate formability cold.

i: Stroke step representing i-th stroke.

j: Iteration counter to decrease the BHF.

n: Number of strokes

$BHF_{i,j}$: Blank holder force of j-th iteration at i-th stroke, unit kN.

$BHF_{0,1}$: Initial blank holder force, unit kN.

B: the constant for checking the wrinkling condition.

D: Distance between the die and the blank holder, unit mm.

T: Thickness deviation.

M: Critical value for checking the thickness deviation.

$L_{\max}$: Total stroke, unit mm.

L_i: Total stroke at i-th stroke, unit mm.

m: Number of the finite elements.

p: Parameter to emphasize the effect of the thickness deviation.

t_0: Initial thickness of the blank, unit mm.

t_i: Thickness of i-th finite element, unit mm.

t_{cri}: Critical value for checking the tearing condition, unit mm.

$t_{\min}$: minimum thickness of the blank, unit mm.

dx_i: Length of the i-th stroke, unit mm.

α: Coefficient to increase the BHF

β: Coefficient to decrease the BHF.

μ: Friction coefficient in the interfaces (blank/blank holder, blank/punch, blank/die, and blank/counter punch).

1. Introduction

Computer Aided Engineering (CAE) is now widely used in engineering fields, such as automotives, aerospace engineering, structural optimization, fluid dynamics, and so on. Physical phenomena can be easily understood using CAE. CAE, including optimization techniques, is also widely applied to sheet forming [1]. In sheet forming, there are many factors that affect the quality of products, such as the Blank Holder Force (BHF), the friction and lubrication conditions of the interface, and the die geometry. Among these factors, BHF plays a key role in the flow of material. In most cases, a constant BHF is applied over the punch stroke. A lower BHF will cause wrinkling due to excessive material flow into the die. In order to prevent wrinkling, a higher BHF needs to be applied. A higher BHF, however, can lead to tearing, thus, it is important to determine the appropriate constant BHF over the punch stroke. Wang et al. [2] suggested that there are four basic windows for BHF formability, as shown in Fig.1. These formability windows represent the relationship between the BHF and the punch stroke.

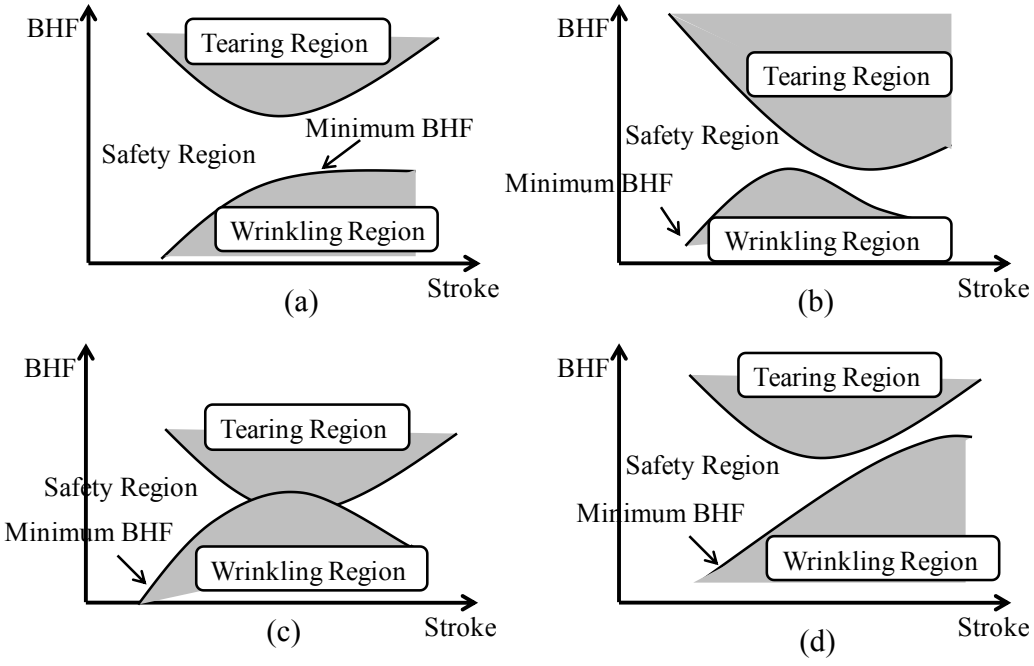

Fig.1 Four basic BHF formability windows [2]

In the formability windows shown in Fig.1(a), it is possible to form a sheet without wrinkling and tearing by applying an appropriate constant BHF. It is impossible, however, to form a sheet with a constant BHF in other cases. In the formability windows shown in Fig.1(b), and (c), particularly, the

Variable Blank Holder Force (VBHF) approach, in which the BHF varies throughout the stroke, is preferable. Numerous researches have been conducted on the VBHF trajectory [2-15]. They can be roughly classified into two categories: those based on a closed-loop type algorithm, and those based on the Response Surface Methodology (RSM). Let us briefly review the use of a closed-loop type algorithm to determine the VBHF trajectory. Wang et al.[2], and Lin et al.[3] developed a closed-loop type algorithm for determining the VBHF trajectory in which a proportional-integral-derivative (PID) controller is introduced. This PID controller was applied to the six separate binders so that six VBHF trajectories could be obtained. Lo and Yang [4] also utilized a PID controller to determine the VBHF trajectory. Sheng et al.[5] developed a closed-loop type algorithm that included a proportional plus integral (PI) controller. Lo and Yang[4], and Sheng et al.[5] utilized the maximum thinning and the flange wrinkling as the state variables. Cao and Boyce [6] utilized the flange wrinkling and the deformed strain instead of the maximum thinning. As the result, the trend of VBHF trajectories predicted by Sheng et al.[5] is in agreement with that predicted by Cao and Boyce. However, towards the end of the punch stroke, the VBHF trajectory predicted by Sheng et al.[5] rapidly increased, while Cao and Boyce's VBHF trajectory decreased, due to the difference of state variables. It is considered that Hardt and Fenn [7], and Sim and Boyce [8] provided the basic idea for the real-time blank holder force control with PI and PID controllers. Other similar researches using a closed-loop type algorithm to obtain VBHF trajectory can be found in Ref.[9,10]. The validity of each of these research efforts has been examined through numerical simulation and experiment [2-5,7]. In these research efforts, the technique that is employed to measure wrinkling and tearing is an important issue for numerical simulation. Thus, a wrinkle is measured by the distance between the die and the blank holder. Wrinkling will develop when the distance between them goes beyond a critical value. In this case, the BHF is increased to suppress wrinkling. Tearing, on the other hand, is measured by the reduction in the thickness. This measuring technique is useful for the numerical simulation.

The other approach for determining the VBHF trajectory is the use of Response Surface Methodology (RSM), which is an approximation technique.

Most of the research using RSM utilizes the Forming Limit Diagram (FLD). In general, two objective functions to prevent wrinkling and tearing are defined by the FLD. The BHF is considered as the design variables. Two objective functions are transformed into one by the weighted sum. Then, the new objective function obtained by the weighted sum is minimized to find the optimal BHF. Chengzhi et al. [16] developed the Adaptive Response Surface Methodology (ARSM) to determine the optimal spatial VBHF, and have applied it to rectangular box deep drawing. Jakumeit et al. [11] defined four objective functions. They employed the Kriging to approximate the objective functions and determined the VBHF trajectory. Wei and Yuying [17] also defined four objective functions: (1) to prevent tearing, (2) to prevent wrinkling, (3) to minimize stretching, and (4) to minimize thickness deviation. Using this approach, they determined the optimal spatial VBHF. Researches to determine the spatial VBHF with RSM can be found in Ref.[18-23].

Other approaches for determining the VBHF trajectory, which employ the Neural Network Method and the Auto-Regressive Moving-Average model (ARMA), can be found in Ref.[12,13]. The VBHF approach can also be also applied to the reduction of springback [14].

In this paper, a simple closed-loop type algorithm is developed for determining the VBHF trajectory. This algorithm is roughly divided into two phases. The objective of first phase of the algorithm is to prevent wrinkling. A lower BHF is employed at start, and then, it is gradually increased to suppress wrinkling. In the first phase, a higher BHF can be attained. However, it might cause tearing. This is why, the second phase is introduced. The objective of the second phase is to reduce the BHF by considering the thickness deviation of the blank. By reducing the BHF attained in the first phase, the risk of tearing is reduced. In the second phase, the risk of wrinkling is constantly checked by the reduction of the BHF. The proposed algorithm is applied to square cup deep drawing. LS-DYNA, which is one of the dynamic explicit Finite Element Analysis (FEA) codes, is employed in the numerical simulation. In order to examine the validity of the proposed algorithm, an experiment was conducted using a hybrid AC servo press belonging to the KOMATSU Industries Corp..

The remainder of this paper is organized as follows: In section 2, the finite element models are described briefly. In addition, some conditions regarding wrinkling and tearing are also described. In section 3, the development of the VBHF algorithm for considering the thickness deviation is presented. The results of the numerical simulation by the proposed algorithm are presented in section 4. Through numerical simulation, the validity of the proposed algorithm is examined.

2. FEA Models and Some Conditions in the Numerical Simulation

2.1 Finite Element Models and Material Properties

The molding of a square cup deep drawing in the experiment is shown in Fig.2(a), and its dimensions are shown in Fig.2(b). A constant BHF (=100 kN) was applied to obtained the result shown in Fig.2(a). In this case, no wrinkling or tearing can be observed.

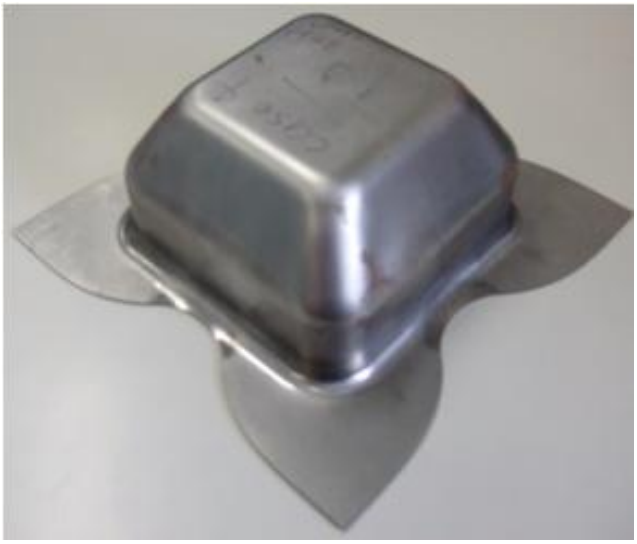

Fig.2(a) Molding in experiment

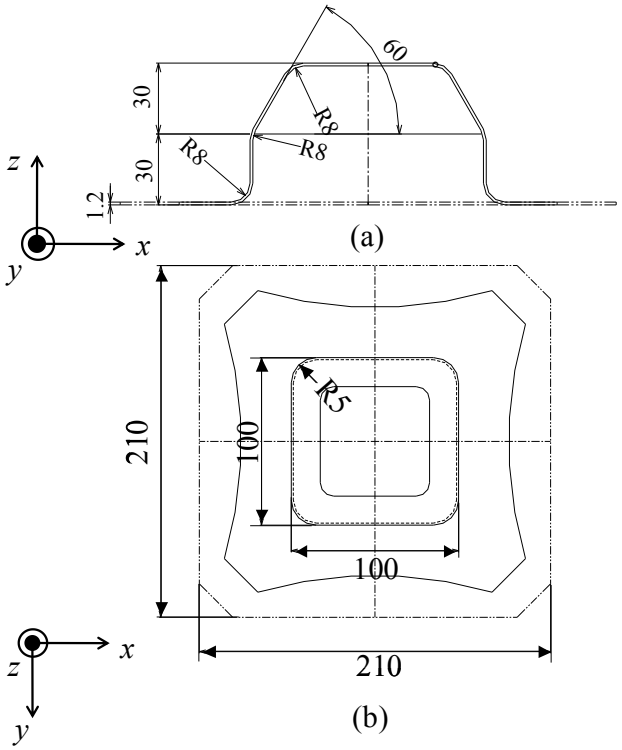

Fig.2(b) Dimensions of molding

In the numerical simulation, LS-DYNA is used. The finite element models of a square cup deep drawing are shown in Fig.3. The element type and the number of finite elements are shown in Table 1. Friction coefficient μ in the interfaces (blank/blank holder, blank/punch, blank/die, and blank/counter punch) is set to 0.1. The blank size is 185 mm x 185 mm, and the initial thickness is 1.20 mm. Considering the symmetry, one fourth model is employed in the numerical simulation as shown in Fig.3. Thus, a blank size of 92.5 mm x 92.5 mm is employed in the numerical simulation. A Belyschko-Tsay shell element with seven integration points across the thickness is used for the shell mesh of the blank. The penalty coefficient for contact (blank/blank holder, blank/punch, blank/die, and blank/counter punch) is set to 0.10. The rigid element is employed to counter punch, die, blank holder, and punch, as listed in Table 1. These material properties such as the density and the young's modulus are the same of blank. However, in the numerical simulation, the rigid elements (counter punch, die, blank holder, and punch) are not deformable.

Table 1 Element type and number of finite elements

	Element type	Number of finite elements
Counter punch	Rigid	120
Die	Rigid	924
Blank	Shell (Belytschko-Tsay)	2116
Blank holder	Rigid	432
Punch	Rigid	962

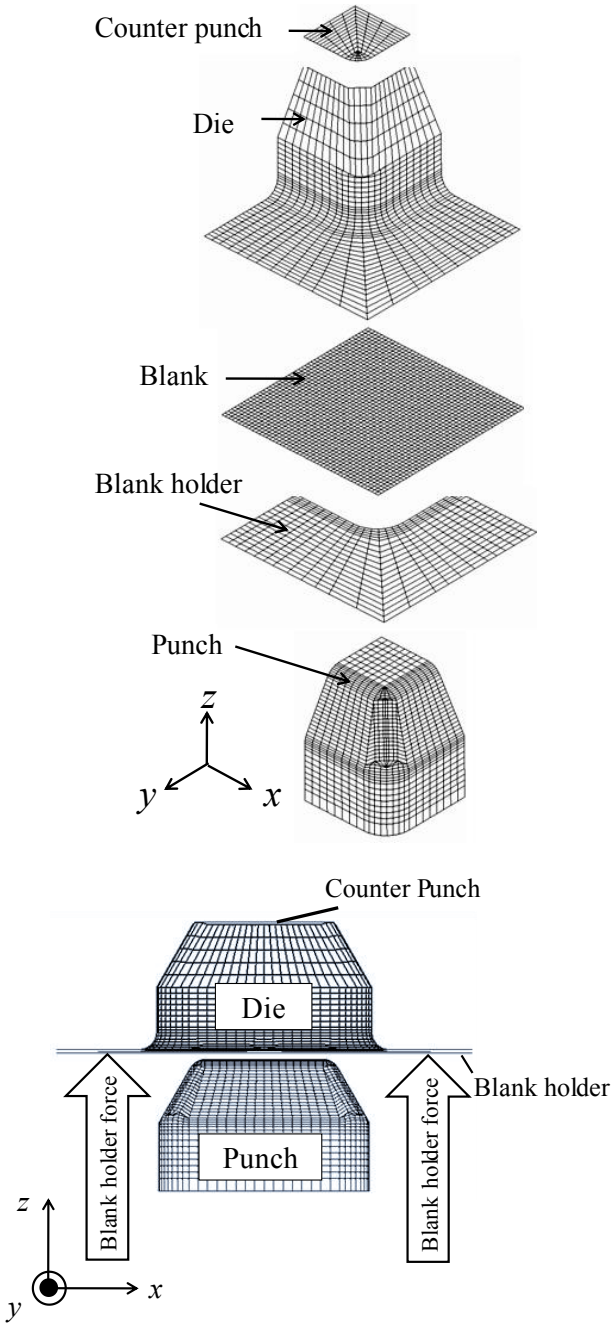

Fig.3 Finite element models

Steel Plate Formability Cold (SPFC) 440 was selected as the test material. The material properties considered through the experiment are shown in Table 2.

Table 2 Material properties of SPFC440

Density: ρ [kg/mm^3]	7.84×10^{-6}
Young's Modulus: E [MPa]	2.06×10^{5}
Poisson's Ratio: ν	0.3
Yield Stress: σ_Y [MPa]	353
Tensile Strength: σ_T [MPa]	479
Normal Anisotropy Coefficient: r	0.98
Strain Hardening Coefficient: n	0.189

The relationship of stress-strain is approximately obtained from the database in LS-DYNA as follows:

$$\sigma = 793\varepsilon^{0.189} \tag{1}$$

A numerical simulation was carried out to examine the validity of the FE model. A constant BHF (= 100 kN) was applied. Comparative results of the numerical simulation and experiment are shown in Fig.4. In addition, the errors in the length are also shown in Table 3.

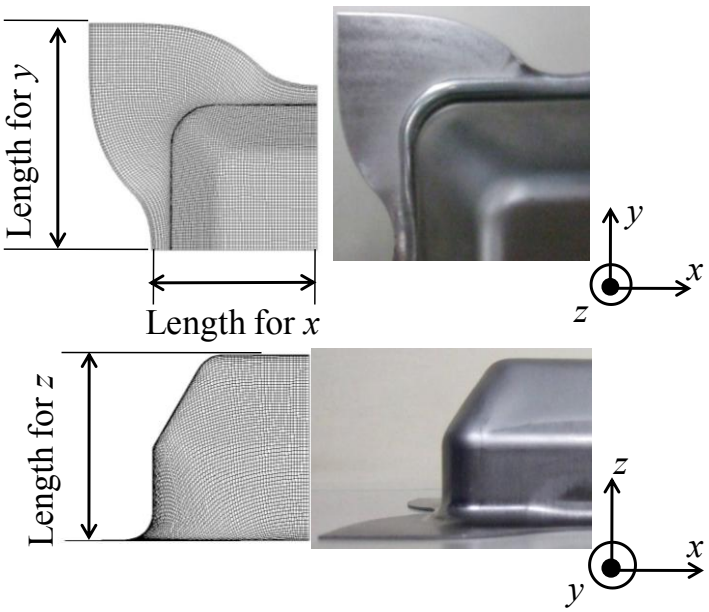

Fig.4 Comparison of the numerical simulation and the experiment

Table 3 Errors in length

Error for x-direction	3.3 [%]
Error for y-direction	0.1 [%]
Error for z-direction	1.2 [%]

2.2 Motion Setting

As shown in Fig.3, the punch is fixed and the BHF is applied in the positive *z*-direction. The counter punch and the die drop to the negative *z*-direction. At the bottom dead centre, the counter punch, the die, and the blank holder move upwards. The motions of these three items in the experiment are shown in Fig.5. In the numerical simulation, the same data are employed. The initial velocity is v_{init} = 267 mm/s, and the maximum velocity is v_{max} = 359 mm/s.

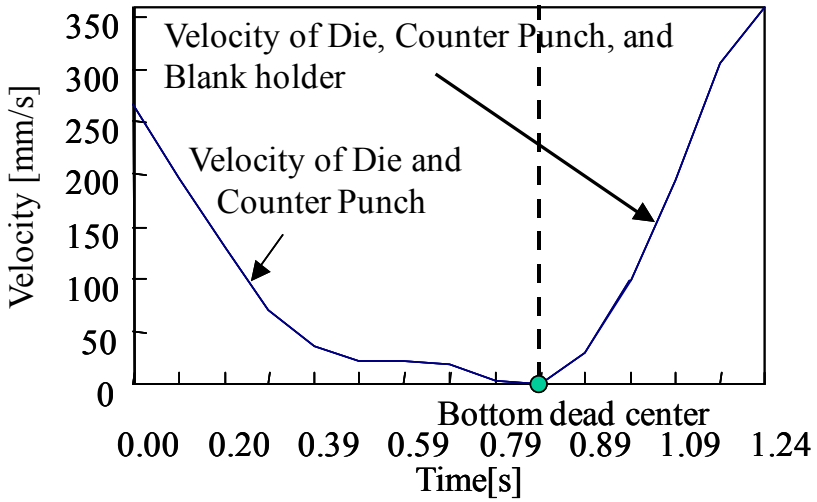

Fig.5 Motion of the die, blank holder, and counter punch

2.3 Wrinkling Condition

Wrinkling in the numerical simulation and in the experiment is shown in Figs.6 and 7. In both cases, a constant BHF (= 20 kN) was applied.

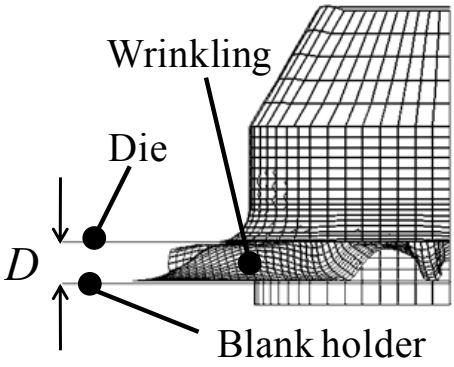

Fig.6 Wrinkling in numerical simulation

Fig.7 Wrinkling in experiment

It is apparent from Fig.6 that the distance D between the die and the blank holder is larger than the initial thickness t_0 when wrinkling occurs. In order to suppress the wrinkling, the BHF is increased. Referring to past researches [2,3,5], the following condition is adopted in order to measure the wrinkling.

$$D > B \times t_0 \rightarrow Wrinkling \tag{2}$$

where B (>1) in Eq.(2) is the constant.

2.4 Tearing Condition

Tearing occurs when the thickness is smaller than the critical value t_{cri} [5]. Thus, the tearing condition is given as follows:

$$t_i < t_{cri} \rightarrow Tearing \quad (i = 1, 2, \cdots, m) \tag{3}$$

where m denotes the number of finite elements in the blank, and t_i represents the thickness of the i-th finite element.

3. A Closed-loop Type Algorithm for the VBHF Trajectory Considering the Thickness Deviation

3.1 A Closed-loop Type Algorithm

In this section, a simple closed-loop type algorithm for determining the VBHF trajectory is explained. First, the algorithm for determining the VBHF trajectory is shown in Fig.8.

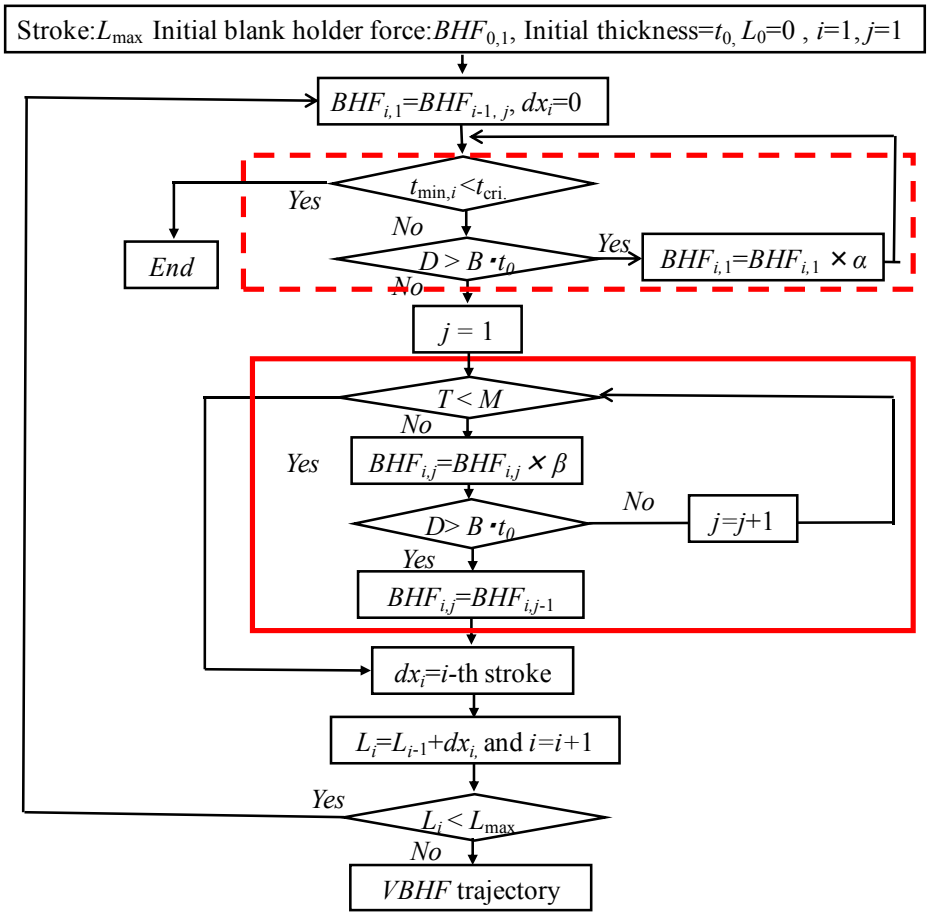

Fig.8 A closed-loop type algorithm for determining the VBHF trajectory

The proposed algorithm is roughly divided into two phases. The aim of the first phase is to prevent wrinkling and tearing (the rectangle inside the dashed line in Fig.8), and the aim of second phase is to consider the thickness deviation (the rectangle inside the solid line in Fig.8). For the sake of simplicity, the first phase is called the wrinkling phase, and the second phase is called the thickness deviation phase. Total stroke L_{max} is partitioned into n stroke. dx_i represents the length of the i-th stroke, and $BHF_{i,j}$ denotes the BHF at the i-th stroke. j expresses the iteration counter, which plays an important role in the thickness deviation phase.

$BHF_{0,1}$, which would cause wrinkling, is assumed to be the initial BHF. The wrinkling phase is considered. When the tearing condition expressed by Eq.(3) is satisfied, the algorithm is terminated. Otherwise, the wrinkling condition described in section 2.3 is examined. If the wrinkling condition expressed by Eq.(2) is satisfied, the BHF is increased in order to suppress the wrinkling.

$$BHF_{i,1} = BHF_{i,1} \times \alpha \quad (\alpha > 1) \tag{4}$$

where α is the coefficient to increase the BHF. In this phase, no wrinkling can be observed. In the wrinkling phase, local information (the distance between the die and the blank holder) is employed in order to measure the wrinkling. Next, we move to the thickness deviation phase.

The aim of this next phase is to examine the thickness deviation of the blank. To this end, global information is considered. The thickness deviation T is defined as follows:

$$T = (\sum_{i=1}^{m} (t_i / t_0 - 1)^p)^{1/p} \tag{5}$$

where t_i represents the thickness of the i-th element, t_0 denotes the initial thickness, and p is the parameter to emphasize the effect of Eq.(5). In the RSM approach, Eq.(5) is often employed [19-21]. In this paper, p is set to 2 [20]. In addition, iteration counter j is introduced in the thickness deviation phase. When T is less than M which is the critical value in the thickness deviation, the BHF and dx_i at the i-th stroke are determined. Otherwise, the BHF is decreased as follows:

$$BHF_{i,j} = BHF_{i,j} \times \beta \quad (0 < \beta < 1) \tag{6}$$

where β is the coefficient to decrease the BHF. Although the decrement of the BHF will lead to wrinkling, the development of wrinkling is constantly checked in this phase ($D > B \times t_0$). When wrinkling can be observed in this phase, $BFH_{i,j\text{-}1}$ is taken at the i-th stroke. To better understand this phase, we provide an illustrative example in Fig.9.

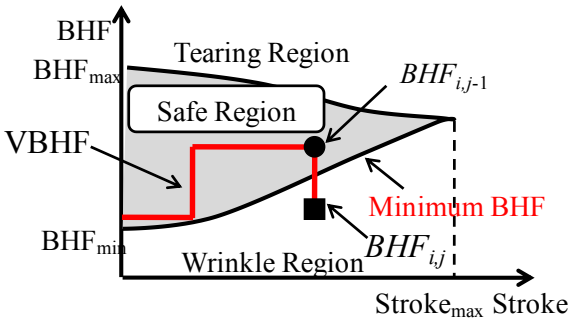

Fig.9 An illustrative example of VBHF

In Fig.9, the black dot and the black square represent the BHF of the j-1-th and j-th iterations at the i-th stroke, respectively. In this example, wrinkling cannot be obserbed at the j-1-th iteration, where $BHF_{i,j\text{-}1}$ is applied. On the other hand, wrinkling can be observed at the j-th iteration, where $BHF_{i,j}$ is applied. In this case, $BHF_{i,j\text{-}1}$ is taken as the BHF at the i-th stroke, and dx_i is also determined. The VBHF trajectory can be obtained by iterating the above two phases.

The characteristics of the proposed algorithm can be summarized as follows:

(1) The proposed algorithm is very simple and is easy to implement.

(2) In past researches on closed-loop type algorithms, local information such as the distance between the die and the blank holder, and the thickness of the tearing, can be used. In the proposed algorithm, this local information can also be included, and in addition, the thickness deviation is employed as global information. Therefore, both local and global information can be used in order to obtain the VBHF trajectory.

3.2 Parameters in the Algorithm

The proposed algorithm shown in Fig.8 requires five parameters. Thus, (1) α : the coefficient to increase the BHF, (2) β : the coefficient to decrease the BHF, (3) B: the constant for checking the wrinkling condition, (4) t_{cri}: the critical value for checking the tearing condition, and (5) M: the critical value for checking the thickness deviation.

4. Numerical Simulation

The validity of the proposed algorithm in this paper is examined through numerical simulation. The parameters in the algorithm are listed in Table 4.

Table 4 Parameter settings

α	1.2
β	0.8
B	1.2
t_{cri}	$0.75\times t_0$
M	2.5

The total length of stroke $L_{\max}$ is 62 mm, and $L_{\max}$ is partitioned into 125 stroke. In section 4.1, the lower BHF is taken as the initial BHF. In section 4.2, the higher BHF is taken as the initial BHF. In section 4.3, different values of parameter M are employed in order to examine upon the effect of the VBHF trajectory.

4.1 Initial blank holder force=20 kN

The initial BHF is set to 20 kN, which causes wrinkling, as described in section 2.3. The algorithm is applied to the SPFC440. The VBHF trajectory

obtained is shown in Fig.10, and the final result with the VBHF trajectory is also shown in Fig.11.

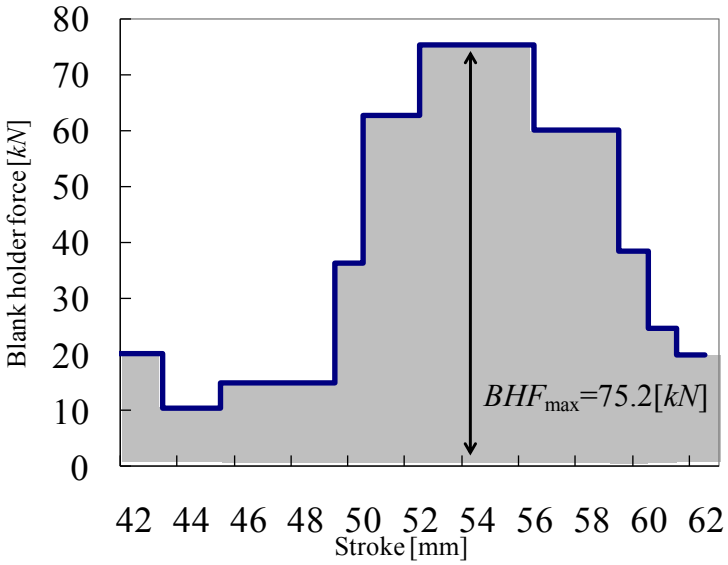

Fig.10 VBHF trajectory at initial BHF=20 kN

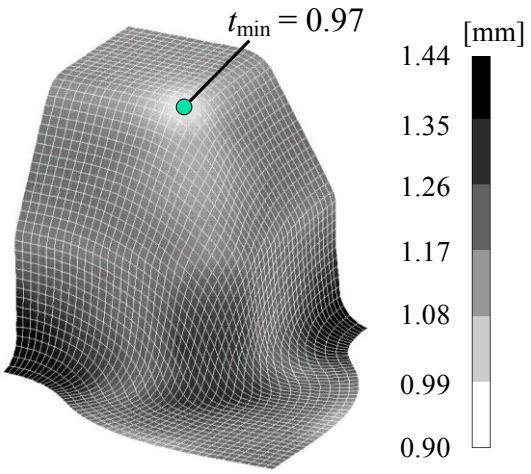

Fig.11 Molding by VBHF in the simulation

The minimum thickness is observed at the punch corner, and is t_{min} = 0.97 mm. This minimum value is greater than t_{cri} (= 0.90 mm). Thus, no wrinkling or tearing can be observed with the proposed algorithm.

The gray area in Fig.10 is considered to represent the forming energy. Next, the forming energy with the VBHF trajectory is calculated. In order to compare the forming energy with the VBHF trajectory, two constants for BHF are used. One is BHF = 75.2 kN, which is the maximum BHF with the VBHF trajectory. The other is BHF=100 kN, as shown in Fig.2(a), a setting at which no wrinkling or tearing can be observed. The values for the forming energy are listed in Table 5.

Table 5 Comparison of forming energy

	Forming energy [kN·mm]
BHF=100 [kN]	6200
BHF=75.2 [kN]	4662
VBHF	1655

It is apparent from Table 5 that the VBHF can drastically reduce the forming energy, as compared to a constant BHF.

4.2 Initial blank holder force=100 kN

Fig.2(a) shows the result obtained with the constant BHF = 100 kN. The proposed algorithm starts at a lower BHF. In the previous section, the initial BHF was set to 20 kN. In this section, the initial BHF is set to 100 kN. In this case, the VBHF trajectory with the proposed algorithm is shown in Fig.12.

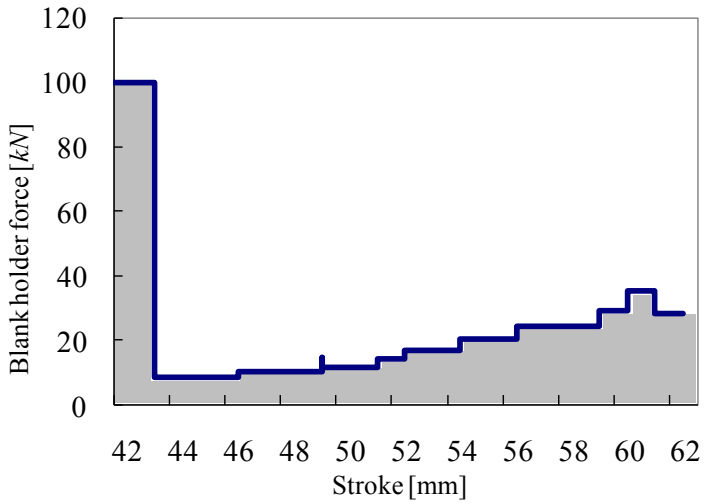

Fig.12 VBHF trajectory at initial BHF=100 kN

It is clear from Fig.12 that the BHF is drastically reduced as the stroke proceeds. The BHF is then gradually increased. In addition, the maximum BHF after the stroke = 44 mm does not attain the force of the initial BHF. This implies that the wasted forming energy is included in the case of the constant BHF=100 kN, and the VBHF approach can reduce the forming energy.

4.3 Parameter M and VBHF trajectory

It is clear from Eq.(5) that T has no dimensions. As the result, the parameter M has also no dimensions. The parameter M, which is the critical value

in the thickness deviation, affects the VBHF trajectory. This critical value M is determined through the numerical simulations in this paper, and there are no guidelines to determining the critical value M in advance. In this section, different critical values of M are used in order to qualitatively examine their effect upon the VBHF trajectory. Three critical values are used. Thus, $M = 2.0$, $M = 2.5$, and $M = 3.0$. The VBHF trajectories for each critical value are shown in Fig. 13.

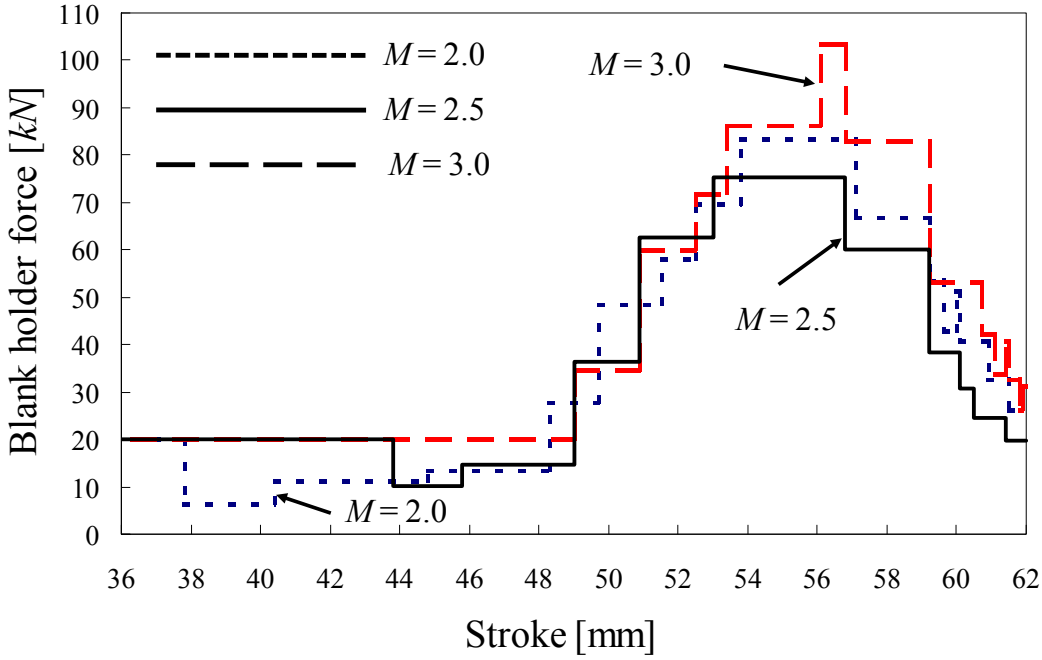

Fig.13 VBHF trajectories for three critical values M

5. Experiment

In this section, the validity of the proposed algorithm is examined through an experiment. The VBHF trajectory was obtained through a numerical simulation, and the experiment was conducted based on this VBHF trajectory. In the experiment, a servo press H1F, which is a hybrid AC servo press belonging to the KOMATSU Industries Corp., was used. SPFC440, whose material properties were presented in Table 2, was used as the blank.

5.1 Initial blank holder force=20 kN

The VBHF trajectory used in the experiment is shown in Fig. 14, in which the solid line and dashed line represent the VBHF trajectory in the experiment and in the numerical simulation, respectively.

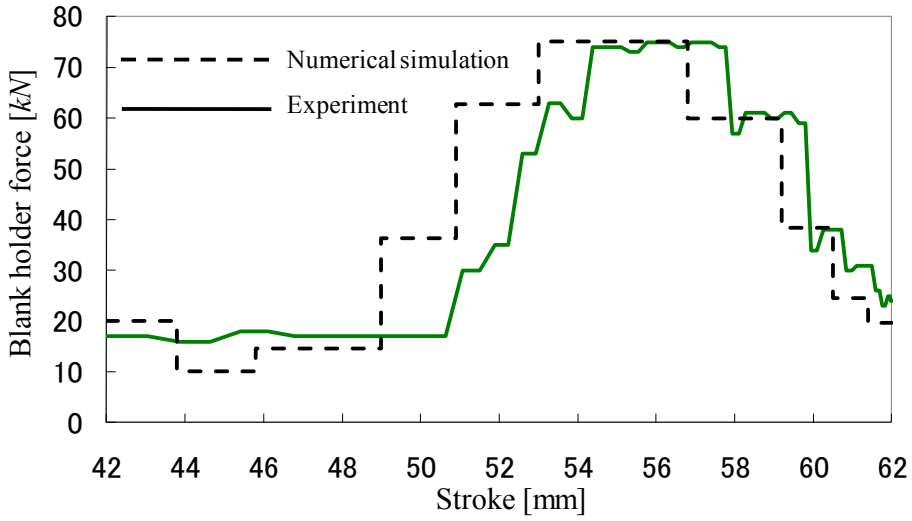

Fig.14 VBHF trajectory (solid line) in the experiment

The final result of the experiment is shown in Fig.15. The dimensions as shown in Fig. 4 are also summarized in Table 6. In addition, the thickness at some points shown in Fig.16, at which tearing often occurs, is measured. The result between the numerical simulation and the experiment is listed in Table 7.

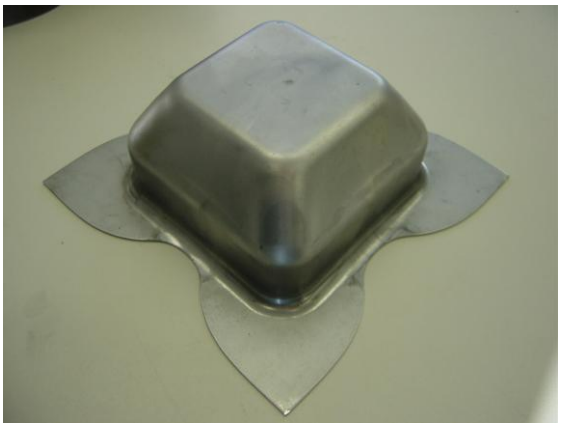

Fig.15 The square cup deep drawing in the experiment (Initial BHF=20 kN)

Table 6 Comparison of the dimensions between the simulation and the experiment

	x	*y*	*z*
Simulation [mm]	54.8	77.2	59.0
Experiment [mm]	57.0	77.6	59.2
Error [%]	3.9	0.5	0.3

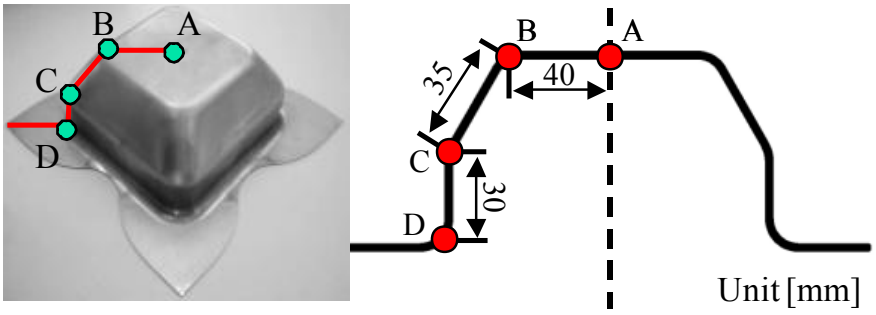

Fig.16 Measuring points of the thickness

Table 7 Comparison of the thickness between simulation and the experiment

Measuring point	A	B	C	D
Simulation [mm]	1.142	0.956	1.108	1.296
Experiment [mm]	1.146	0.958	1.088	1.301
Error [%]	0.35	0.21	1.84	0.38

5.2 Initial blank holder force=100 kN

The VBHF trajectory used in the experiment is shown in Fig. 17, in which the solid line and dashed line represent the VBHF trajectory in the experiment and in the numerical simulation, respectively.

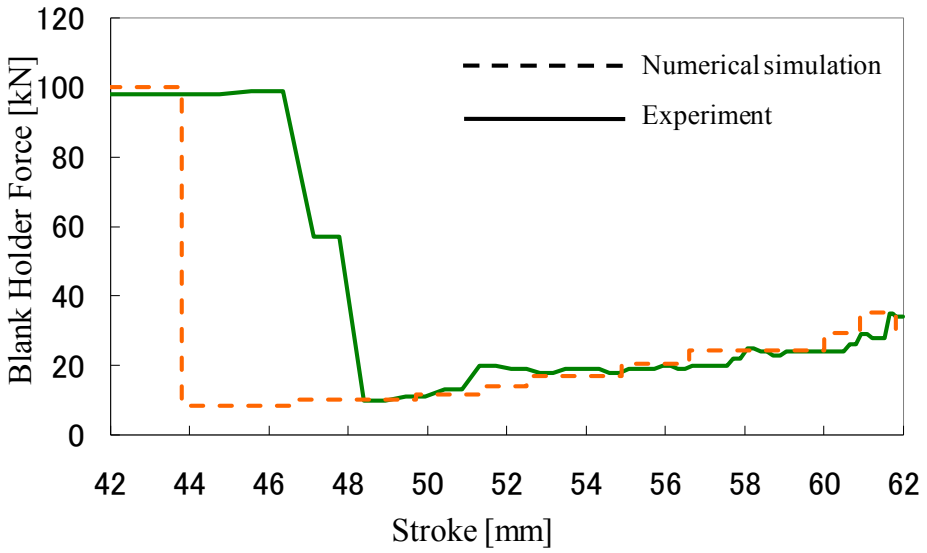

Fig.17 VBHF trajectory (solid line) in the experiment

The final result of the experiment is shown in Fig.18. The dimensions as shown in Fig. 4 are also summarized in Table 8. The thickness at some points shown in Fig.16, at which tearing often occurs, is measured. The result between the numerical simulation and the experiment is listed in Table 9.

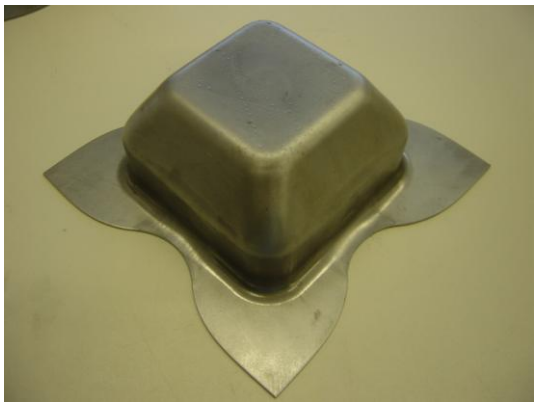

Fig.18 The square cup deep drawing in the experiment (Initial BHF=100 kN)

Table 8 Comparison of the dimensions between the simulation and the experiment

	x	*y*	*z*
Simulation [mm]	54.7	77.4	59.0
Experiment [mm]	57.0	77.5	59.3
Error [%]	4.0	0.1	0.5

Table 9 Comparison of the thickness between simulation and the experiment

Measuring point	A	B	C	D
Simulation [mm]	1.117	0.933	1.127	1.311
Experiment [mm]	1.131	0.794	1.08	1.312
Error [%]	1.24	17.51	4.35	0.08

6. Discussions

In the numerical simulations, no wrinkling and tearing can be observed by the VBHF trajectories with the proposed algorithm. It has been clear that VBHF trajectories with the proposed algorithm can drastically reduce the forming energy in comparison with the application of the constant BHF. In addition, a high BHF was taken as the initial BHF. In such a case, it was apparent that the wasted forming energy is included into the process of forming. Therefore, the initial BHF was drastically reduced as the stroke proceeded, and the BHF was gradually increased. The maximum BHF by the VBHF did not reach the level of the initial BHF. We consider that this result confirms the validity of forming with the minimum BHF, as suggested by Obermeyer and Majlessi [15]. Three different values of the parameter *M* are employed in order to examine the effect on the

VBHF trajectory. Through numerical simulations, it is qualitatively clear from Fig.13 that similar VBHF trajectories can be obtained. Therefore, the BHF is gradually increased as the punch stroke proceeds. The VBHF trajectories have the extreme, and the BHF is decreased in the final stage of the punch stroke. Then, the experiment was conducted in order to examine the validity of the proposed algorithm. It is clear from Figs.15 and 18 that no wrinkling or tearing can be observed in the physical results obtained in the experiment. A high degree of accuracy of in regard to dimensions and thickness was also obtained. The error at point B in Table 9 is larger than the error in the other measuring points. A high BHF is applied, and then the BHF is gradually decreased in the experiment, while a BHF is rapidly is decreased in the numerical simulation. It is considered that the delay of the VBHF in the experiment may cause the large error at point B. The quick decrement of BHF is difficult in the present servo press. To reduce the errors between numerical simulation and experiment, the delay should be minimized. It is expected that the control system of the present servo press will be improved to minimize the delay. However, we consider that the results between numerical simulations and experiments coincide. Therefore, the validity of the proposed algorithm has been confirmed through numerical simulations and experiments.

7. Conclusions

In this paper, a simple closed-loop type algorithm for the VBHF trajectory was developed, and it was applied to a square cup deep drawing. The proposed algorithm can be roughly divided into two phases: the wrinkling phase and the thickness deviation phase. In the wrinkling phase, the BHF is increased in order to suppress wrinkling. In the thickness deviation phase, the BHF is decreased. The proposed algorithm begins at a low BHF. This is in conformance with the suggestion of Obermeyer and Majlessi [15] regarding the importance of sheet forming by using minimum BHF. An FE model was constructed on basis of the experiment. Numerical simulation was carried out in order to examine the validity of the proposed algorithm. Through the numerical simulation, it was found that the forming energy achieved with the VBHF could be reduced drastically, as compared to the application of a constant BHF. The validity of the proposed algorithm was evaluated through numerical examples.

References:

1. Gantar, G., Pepelnjak, T., Kuzman, K. (2002) Optimization of sheet metal forming process by the use of numerical simulations, J Mater Process Technol, 130-131: 54-59
2. Wang, W.R., Chen, G.L., Lin, Z.Q., Li, S.H. (2007) Determination of optimal blank holder force trajectories for segmented binders of step rectangle box using PID closed-loop FEM simulation, Int J Adv Manuf Technol, 32: 1074-1082
3. Lin, Z.Q., Wang, W.R., Chen, G.L. (2007) A new strategy to optimize variable blank holder force towards improving the forming limits of aluminum sheet metal forming, J Mater Process Technol, 183: 339-346
4. Lo, S.W., Yang, T.C. (2004) Closed-loop control of the blank holding force in sheet metal forming with a new embedded-type displacement sensor, Int J Adv Manuf Technol, 24: 553-559
5. Sheng, Z.Q., Jirathearanat, S., Altan, T. (2004) Adaptive FEM simulation for prediction of variable blank holder force in conical cup drawing, J Mach Tools Manuf, 44: 487-494
6. Cao, J., Boyce, M.C. (1997) A predictive tool for delaying wrinkle and tearing failures in sheet metal forming, ASME J Eng Mater Technol, 119: 354-365
7. Hardt, D.E., Fenn, R.C. (1993) Real-Time control of sheet stability during forming, ASME J Eng Ind, 115: 299-308
8. Sim, H.B., Boyce, M.C. (1992) Finite element analyses of real-time stability control in sheet forming processes, ASME J Eng Mater Technol, 114: 180-188
9. Traversin, M., Kergen, R., (1995) Closed-loop control of the blank-holder force in deep-drawing: finite-element modeling of its effects and advantages, J Mater Process Technol, 50: 306-317
10. Hsu, C.W., Ulsoy, A.G., Demeri, M.Y. (2000) An approach for modeling sheet metal forming for process controller design, ASME J Manuf Sci Eng, 122: 717-724
11. Jakumeit, J., Herdy, M., Nitsche, M. (2005) Parameter optimization of the sheet metal forming process using an iterative parallel Kriging algorithm, Struct Multidisciplinary Optim, 29: 498-507
12. Krishnan, N., Cao, J. (2003) Estimation of optimal blank holder force trajectories in segmented binders using an ARMA model, ASME J Manuf Sci Eng, 125: 763-770
13. Cao, J., Kinsey, B., Solla, S.A. (2000) Consistent and minimal springback using a stepped binder force trajectory and neural network control, ASME J Eng Mater Technol, 122: 113-118
14. Liu, G., Lin, Z., Xu, W., Bao, Y. (2002) Variable blankholder force in U-shaped part forming for eliminating springback error, J Mater Process Technol, 120: 259-264
15. Obermeyer, E.J., Majlessi, S.A. (1998) A review of recent advances in the application of blank-holder force towards improving the forming limits of sheet metal parts, J Mater Process Technol, 75: 222-234
16. Chengzhi, S., Guanlong, C., Zhongqin, L. (2005) Determining the optimum variable blank-holder forces using adaptive response surface methodology (ARSM), Int J Adv Manuf Technol, 26: 23-29

17. Wei, L., Yuying, Y. (2008) Multi-objective optimization of sheet metal forming process using pareto-based genetic algorithm, J Mater Process Technol, 208: 499-506
18. Jansson, T., Nilsson, L., Redhe, M. (2003) Using surrogate models and response surface in structural optimization -with application to crashworthiness design and sheet metal forming, Struct Multidisciplinary Optim, 25: 129-140
19. Wang, H., Li, G.Y., Zhong, Z.H. (2008) Optimization of sheet metal forming processes by adaptive response surface based on intelligent sampling method, J Mater Process Technol, 197: 77-88
20. Breitkopf, P., Naceur, H., Rassineux, A., Villon, P. (2005) Moving least squares response surface approximation: Formulation and metal forming applications, Comput Struct, 83: 1411-1428
21. Wang, H., Li, E., Li, G.Y. (2008) Optimization of drawbead design in sheet metal forming based on intelligent sampling by using response surface methodology, J Mater Process Technol, 206: 45-55
22. Wang, L., Lee, T.C. (2005) Controlled strain path forming process with space variant blank holder force using RSM method, J Mater Process Technol, 167: 447-455
23. Naceur, H., Ben-Elechi, S., Batoz, J.L. (2008) Knopf-Lenoir C., Response surface methodology for the rapid design of aluminum sheet metal forming parameters, Mater Des, 29: 781-790